DAΦNE TECHNICAL NOTE

INFN - LNF, Accelerator Division

Frascati, March 12, 1993

Note: **G-18**

MULTIBUNCH INSTABILITIES IN DAΦNE:
LONGITUDINAL AND TRANSVERSE COHERENT FREQUENCY SHIFT

M. Migliorati, L. Palumbo

1. Introduction

The beam-cavity interaction due to the parasitic modes of an RF cavity, can lead to a strong instability expecially in the case of high current colliders, such as DAΦNE. The analysis of the dynamics of k_b equispaced bunches interacting with the long range wakefields is performed by computing the coherent frequency shift predicted by the Sacherer theory [1] or by equivalent analysis given by Pellegrini-Wang, Laclare, Besnier and others[2]. The instability rise time can be obtained from the real part of this complex frequency shift derived by considering the coupling of the beam with the HOMs.

In this note we use the Laclare formalism of the multibunch instability, both longitudinal and transversal, in the simple case of a single resonant mode coupling the bunch motion, for evaluating the rise times of the dipole and quadrupole modes for the two cavity shapes proposed for DAΦNE, namely the *rounded* and that with *nose-cones*.

Let us consider a Gaussian bunch. Its stationary distribution $g_o(\tau)$ in the phase space is given by:

$$g_o(\tau) = \frac{1}{2\pi\sigma_\tau^2} \exp\left[-\tfrac{1}{2}\left(\tau/\sigma_\tau\right)^2\right] \qquad (1)$$

where σ_τ is the bunch length in the time domain, and g_o is normalized with respect to polar coordinates, that is

$$\int_o^{2\pi} d\psi \int_o^{\infty} g_o(\tau)\tau d\tau = 1 \qquad (2)$$

Any perturbation of the bunch distribution is developed as sum of multipole coherent modes $\Delta\Psi_m$. Under the effect of long range wakefields the coherent mode of oscillation "m" (m = 1 dipole, m = 2 quadrupole and so on)

can grow or decay in amplitude:

$$\Delta\Psi_m = g_m(\tau)\exp[j(\omega_{cm} - m\omega_s)] \tag{3}$$

where g_m is the perturbation amplitude, ω_s is the unperturbed synchrotron frequency, and ω_{cm} - $m\omega_s$ is a complex frequency shift.

In the frequency spectrum, the coherent mode of perturbation *"m"* will have an amplitude at the frequency $\omega=p\omega_o+\omega_{cm}$, with ω_o the revolution frequency and $-\infty < p < \infty$, proportional to:

$$\sigma_m(p) = j^{-m}\int_o^\infty J_m(p\omega_o\tau)g_m(\tau)\tau\,d\tau \tag{4}$$

where J_m is the Bessel function of the first kind.

If this signal, at frequency $\omega=p\omega_o+\omega_{cm}$, excites resonant fields, described by the impedance $Z(\omega)$, from the linearized Vlasov equation, one derives the following equation[3]:

$$\begin{aligned} &j(\omega_{cm} - m\omega_s)\sigma_m(l) = \\ &= -\frac{m\alpha_c I_o}{\omega_s(E/e)}\sum_p \frac{Z(p\omega_o+\omega_{cm})}{p}\sum_h \sigma_h(p)\int_o^\infty \frac{\partial g_o}{\partial\tau} J_m(p\omega_o\tau)J_m(l\omega_o\tau)d\tau \end{aligned} \tag{5}$$

where I_o is the average beam current, α_c the momentum compaction, E the beam energy, and e the electron charge.

Once the machine impedance and the bunch spectrum of a perturbed beam are known, one can derive the effective impedance seen by the beam and the coherent complex frequency shift of a relative mode.

The customary way of computing the coherent frequency shift considers the bunch spectrum at frequencies

$$\omega_p=(pk_b + n + m\nu_s)\,\omega_o \tag{6}$$

with $1 < n < k_b$, i.e. the spectrum of a bunch with m-pole perturbation executing "natural" oscillations in absence of any growth rate or damping. This procedure leads to the solution of a linear equation system for the unknown ω_{cm}. This is not exactly what is prescribed in Eq.(4) where the impedance has to be computed at frequencies that include the coherent frequency shift. As matter of facts, the system in Eq.(4), is an "eigenvalue" problem for the coherent shifts ω_{cm}. Computing the impedance at the bunch spectrum sidebands (5) leads to an inexact estimate of the growth rates, especially for the cases of high intensity, high Q resonance[4].

2. The case of a single resonator.

Let us assume that there is a single resonant mode coupling the relative bunch motion, at a frequency ω_r and let R and Q be the resonator parameters. In this simple case the system (4) simplifies to only one equation:

$$j(\omega_{cm} - m\omega_s) = -\frac{m\alpha_c I}{\omega_s (E/e)} \frac{Z(p\omega_o + \omega_{cm})}{p} \int_o^\infty \frac{\partial g_o}{\partial \tau} J_m^2(p\omega_o \tau) d\tau \qquad (7)$$

where

$$Z(p\omega_o + \omega_{cm}) = \frac{R}{1 + jQ\left(\frac{p\omega_o + \omega_{cm}}{\omega_r} - \frac{\omega_r}{p\omega_o + \omega_{cm}}\right)} \qquad (8)$$

For simplicity Eq.(6) is given in the compact form:

$$j(\omega_{cm} - m\omega_s) = \theta_m(p) \frac{Z(p\omega_o + \omega_{cm})}{p} \qquad (9)$$

In Fig. 1 we show the behavior of $\theta_m(p)/p$, versus *"p"*, for *m=1, 2, 3* and σ*=3 cm*, computed for DAΦNE.

In the realistic case that $\omega_{cm} << \omega_r$, the impedance can be approximated by :

$$Z(p\omega_o + \omega_{cm}) \approx \frac{R}{1 + \frac{j\omega_{cm}}{\alpha} + jtg(\Phi_r)} \qquad (10)$$

where

$$\alpha = \frac{\omega_r}{2Q} \qquad (11)$$

is the filling rate of the resonant mode, (τ_f *= 1 /* α = filling time) and

$$tg(\Phi_r) = Q\left(\frac{p\omega_o}{\omega_r} - \frac{\omega_r}{p\omega_o}\right) \qquad (12)$$

defines the "detuning" of the resonant mode with respect to the line "*p*" of the bunch spectrum.

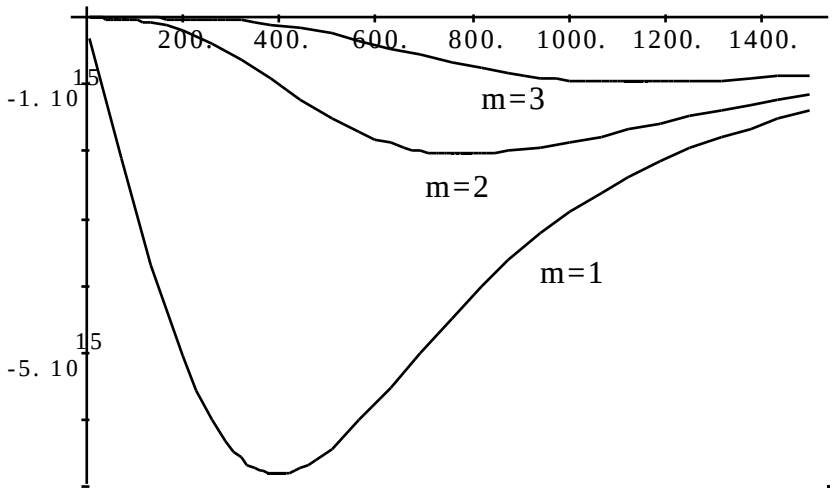

Fig. 1 - DAΦNE : $\theta_m(p)/p$, versus "p", for $m=1, 2, 3$ and $\sigma=3\ cm$.

With these definitions and approximations, the coherent tune shift is obtained by solving the following equation:

$$\omega_{cm}^2 + \left[\alpha tg(\Phi_r) - m\omega_s - j\alpha\right]\omega_{cm} - \alpha\left[m\omega_s tg(\Phi_r) - \frac{\theta_m(p)R}{p} - jm\omega_s\right] = 0 \quad (13)$$

which gives

$$\omega_{cm} = \frac{\alpha}{2}\left[\left(\frac{m\omega_s}{\alpha} - tg(\Phi_r)\right) + j\right] + \\ - \sqrt{\left[-j + \left(tg(\Phi_r) - \frac{m\omega_s}{\alpha}\right)\right]^2 \frac{\alpha^2}{4} + \alpha\left[\left(m\omega_s tg(\Phi_r) - \frac{\theta_m(p)R}{p}\right) - jm\omega_s\right]} \quad (14)$$

where the plus sign has been excluded since leads to unphysical results.

Hereafter we shall consider some relevant cases.

2.1 Dipole modes, (m=1).

The complex frequency shift of the dipole modes excited by a single resonator is given by Eq. (13) with $m=1$. Of particular interest is the on resonance beating case (full coupling) which will be first examined.

a) Full coupling condition:

Let us assume a resonator at $\omega_r = p\omega_o + \omega_s$, we get:

$$tg(\Phi_r) = -\frac{\omega_s}{\alpha} \tag{15}$$

$$\omega_{c1} = \omega_s + j\frac{\alpha}{2}\left[1 - \sqrt{1 + 4\frac{\theta_1 R}{p\alpha}}\right] \tag{16}$$

As expected, in the full coupling condition there is no shift of the real synchrotron frequency, whereas the imaginary shift gives the growth rate of the instability. We recognize in the term

$$\frac{p}{\theta_1 R} = \tau_1 \tag{17}$$

the instability rise time usually obtained from Eq. (4). This rise time is inversely proportional to the beam current I_o times the shunt impedance R. It is interesting to analyze two different regimes.

For $\tau_1 >> \tau_f$, we get:

$$\omega_{c1} \approx \omega_s - j\frac{1}{\tau_1} \tag{18}$$

In this case, therefore, the rise time computed with Eq. (16), can be considered as a fairly good approximation.

Quite different results are obtained in the other case, namely when $\tau_1 << \tau_f$. In fact we get:

$$\omega_{c1} \approx \omega_s - \frac{j}{\sqrt{\tau_1 \tau_f}} \tag{19}$$

The effective rise time τ_{eff} results to be the geometric mean of τ_1 and τ_f, One could argue from the above equation that superconducting cavities, characterized by an extremely long filling time, should be preferred for what concerns multibunch instabilities. This, however, is not exactly true. In fact, expliciting the two terms in the rise time of Eq.(18) we have:

$$\tau_{eff} = \left(\frac{2p}{\theta_1 \omega_r (R_s / Q)}\right)^{\frac{1}{2}} \tag{20}$$

This means that the effective rise time is inversely proportional to the square root of the ratio R/Q. Therefore, by increasing Q keeping R/Q constant, the effective rise time reaches an asymptotic value no more dependent on the cavity filling time.

For short bunches, it is useful to write down the effective rise time in the form:

$$\tau_{eff} = \left(\frac{8\pi (E/e)\nu_s}{I_o \alpha_c} \right)^{\frac{1}{2}} \frac{1}{\omega_r (R_s/Q)^{\frac{1}{2}}} \qquad (21)$$

where ν_s is the synchrotron tune.

In Fig. 2 we plot, as function of Q, the growth rates $\alpha_1 = 1/\tau_1$ and $\alpha_{eff} = 1/\tau_{eff}$ computed for DAΦNE, assuming a sample parasitic resonance with $R/Q=1$, at $\omega_r = 500\ \omega_o + \omega_s$, exciting the motion of 30 bunches of 3 cm length and for a total current 1.4 Ampere. The upper curve is the growth rate $\alpha_1(Q)$ while the lower one is $\alpha_{eff}(Q)$. We note that at high Q's the difference between the two curves becomes larger and larger. In order to verify the correctness of the Eq.(15) we have reported on the same plots the instability growth rates (dots) obtained from the time domain simulation code recently developed[5]. The concordance of the results goes beyond the expectations.

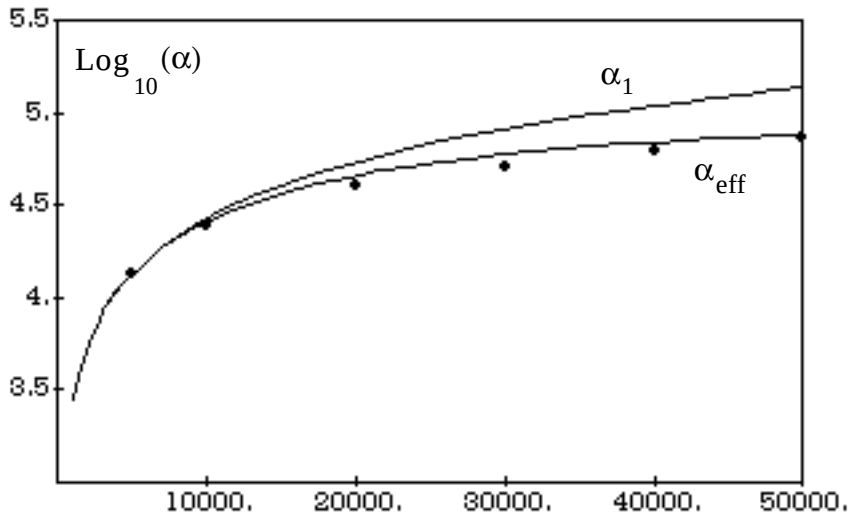

Fig. 2 - DAΦNE Growth rates $\alpha_1(Q)$ and $\alpha_{eff}(Q)$, for an HOM with $R/Q=1$

For the DAΦNE cavity only few HOM's with a relatively high shunt impedance give a τ_{eff} significantly higher than τ_1. In Table I we report the results relative to the HOM's of the "round shape cavity". The rise time of the dipole mode computed with Eq.(18) are given in column 5. We have to remark

that a factor 5 is gained on the mode TM_{011} where we have $\tau_{eff} \approx 11\mu s$ instead of $\tau_1 \approx 2.2\ \mu s$. In column 6 we give the Q values which, in full coupling, lead to a rise time of 100 μs and 200 μs, such to be damped, if considered separately, by the longitudinal feedback system [6]. In Table II we give the same results computed for the the HOM's of the "nose cone cavity". We note that there is an appreciable difference only on the TM011 mode, more favorable for the nose cone cavity. However, once we assume to adopt a HOM's damping system, the overall behavior of the two cavities is not significantly different.

Table I Rise time of the dipole mode (round shape cavity)

Frequency MHz	Q	R/Q	τ	τ_{eff}	$Q_{100\mu s,\ 200\mu s}$
734.42663	51875	13.4847	42 ms	11 µs	1240 620
797.89267	85575	0.0265	47 ms	763 µs	--------
1006.20602	68418	0.00422	15 s	5 ms	--------
1086.43925	68709	0.11035	4.9 ms	219 µs	--------
1163.18159	61292	0.24326	4 ms	119 µs	----28700
1234.49657	73587	1.49657	115 ms	29 µs	9700 4600
1317.27807	60346	0.33961	300 ms	90 µs	44400 21500
1357.49229	74703	1.36814	180 ms	29 µs	10500 5200
1429.05804	62789	0.72471	270 ms	48 µs	20300 10000
1527.46005	65748	0.06644	1.8 s	363 µs	--------
1529.25741	61751	1.88715	74.8 ms	25 µs	7900 3900
1619.86464	74241	0.82329	54 ms	41 µs	18900 9000
1643.96878	67986	1.2874	110 ms	30 µs	12000 5900
1725.0832	79431	0.72091	32 ms	45 µs	22500 11100
1762.6359	69885	2.25743	77 ms	21 µs	7200 3600
1767.80826	73737	0.82520	3.2 ms	41 µs	19800 9700
1800.69538	76277	0.21935	385 ms	119 µs	----37800
1869.62599	76875	0.10493	655 ms	230 µs	--------
1890.1208	64890	0.7321	16 ms	50 µs	23700 11700
1978.9835	78377	0.23656	117 ms	115 µs	----37800
1985.50556	96935	0.18573	3 ms	122 µs	----48500

Table II Rise time of the dipole mode (nose cone cavity)

Frequency MHz	Q	R/Q	τ	τ_{eff}	$Q_{100\mu s,}$	$_{200\mu s}$
703.664	30391	4.033	79 ms	27 µs	4300	2100
1077.551	56920	0.264	137 ms	119 µs	----	27900
1115.394	42102	0.19	1.8 s	198 µs	----	----
1157.494	45723	0.049	1 s	655 µs	----	----
1297.383	56139	0.227	487 ms	131 µs	----	31800
1378.898	51298	0.302	475 ms	110 µs	----	24200
1433.226	61704	0.428	1 ms	74 µs	35000	17000
1461.218	39830	1.4	14 ms	36 µs	10400	5200
1526.019	73465	1.011	112 ms	36 µs	15100	7300
1550.471	50192	0.143	405 ms	225 µs	----	----
1627.805	58302	0.19	1.2 s	156 µs	----	41300
1666.862	54095	1.026	24 ms	39 µs	15100	7500
1755.688	52166	0.804	11 ms	50 µs	19800	9900
1775.060	57886	3.284	56 ms	18 µs	4800	2400
1807.090	37277	0.345	50 ms	138 µs	49500	24200
1910.564	56912	1.531	128 ms	30 µs	11300	5600
1981.762	132261	0.022	5.8 s	650 µs	----	----
1996.561	60832	0.91	196 ms	45 µs	19800	9900
2060.516	60302	0.533	336 ms	72 µs	36000	17600
2316.240	64694	1.092	54 ms	41 µs	19800	9900
2409.977	64745	2.091	40 ms	27 µs	10800	5400
2492.123	66749	2.665	1.6 ms	21 µs	9000	4500
2617.936	49845	0.907	3.2 ms	66 µs	28800	14000
2673.274	70704	2.552	3.6 ms	23 µs	10400	5200

For sake of completeness, we want to stress that the growth rates have been worked out assuming an individual coupling of one sideband with a single resonator. These calculations neglect the superposition of the shunt impedance, of several HOM's on the same relative mode. This effect can enhance (sum of shunt impedances) or reduce (difference of shunt impedance) the coupling. The time simulation code shows, in the presence of the HOM's damping system, that for DAΦNE this effect is generally negligible.

b) Off resonance coupling:

The analysis of the coherent frequency shift (13) for a parasitic resonator moving around a sideband at $\omega = p\omega_0 + \omega_s$ is also interesting. A first problem arising in the calculation of ω_{c1} is the following: as consequence of the coupling to the imaginary part of the impedance the sidebands ω_p, Eq.(5), shifts toward the resonant frequency ω_r of the HOM; this shift leads to a stronger coupling with the resistive impedance and to a further, even though lower, shift of ω_p toward ω_r. Iterating the procedure, every coupled sideband should see, at the end, the maximum shunt impedance. Fortunately, the right expression of ω_{c1} Eq.(13) shows that the sideband finds a new equilibrium frequency, which in the cases of interest, is not significantly far from the unperturbed position.

A sample HOM with Q=10000, R/Q=1 and p=500, has been chosen to compare Eq.(13) with the time domain simulation code. Also in this case the agreement is quite satisfactory, as shown in Figs. 3 and 4 where both the growth rates and frequency shifts predicted by Eq. (13) are reported together with the time domain results.

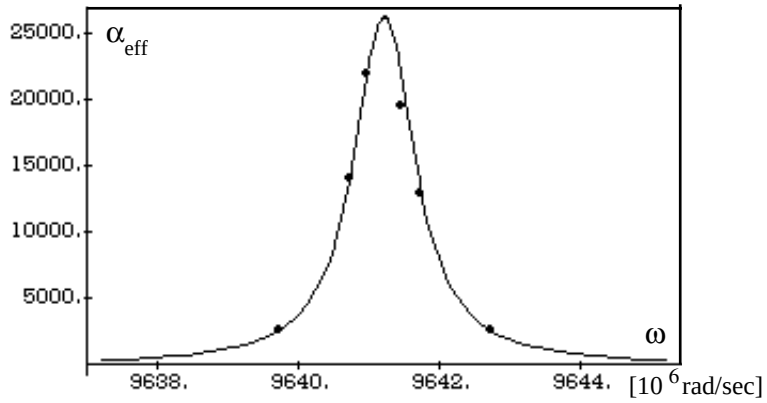

Fig. 3 - DAΦNE: Growth rate $\alpha_{eff}(\omega)$ for R/Q=1, Q=10^4, p=500.

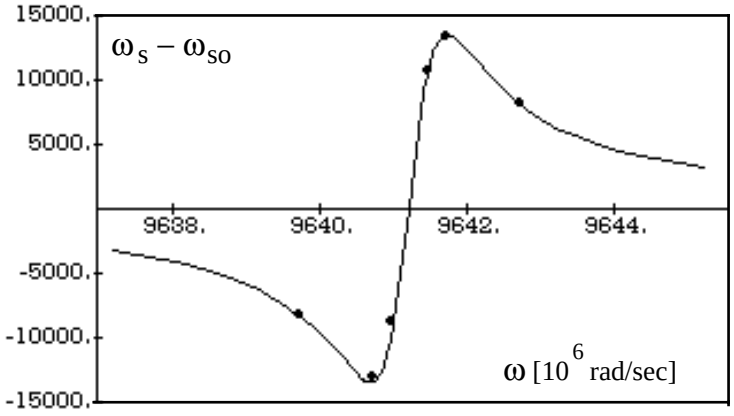

Fig. 4 - DAΦNE: Frequency shift $\Delta\omega_s(\omega_r)$, [rad/s], for R/Q=1, Q=10^4, p=500.

2.2 Quadrupole (m=2) modes.

The resonant modes of the cavity can enhance the amplitude of the m-pole perturbation of the bunch distribution. It is clear that these modes are harmful when the sidebands of a given relative quadrupole mode beat the HOM's close to the resonant frequency. The growth rate can be very high, and unlike the dipole mode, no feedback system is, at moment, foreseen to damp this instability. We can rely only on the reduction of growth rate caused by lowering the *"Q"*, and on the Landau damping.

Analogously to the dipole mode, let us analyze the simple case of a parasitic resonance at the frequency:

$$\omega_r = p\omega_o + 2\omega_s \tag{21}$$

which corresponds to a detuning angle:

$$tg(\phi_r) = -\frac{2\omega_s}{\alpha} \tag{22}$$

and a coherent frequency shift:

$$\omega_{c2} = 2\omega_s + j\frac{\alpha}{2}\left[1 - \sqrt{1 + 4\frac{\theta_2 R}{p\alpha}}\right] \tag{23}8$$

We recognize in the term

$$\tau_2 = \frac{p}{\theta_2 R} \tag{24}$$

the rise time one obtains in the perturbation approximation, which works rather well under the condition $\tau_2 >> \tau_f$, for which we find:

$$\omega_{c2} \approx 2\omega_s - \frac{j}{\tau_2} \tag{25}$$

while is inaccurate in the other case $\tau_2 << \tau_f$ for which we have:

$$\omega_{c2} \approx 2\omega_s - \frac{j}{\sqrt{\tau_2 \tau_f}} \tag{26}$$

In Table IIIa and IIIb, for both cavities, we give the growth times for each HOM assumed to be beaten at the resonant frequency. In the last column we give the Q corresponding to a shunt impedance of 500 Ω, impedance limit obtained from the stability diagram due to the Landau Damping (see next Section).

Table IIIa Rise times of the quadrupole modes (round shape cavity)

ω_r(MHz)	R/Q	Q_o	$\tau_{2,eff}$	Q (500 Ω)
734.42	13.5	52000	43.0 µs	40
797.89	0.02	85000	5.6 ms	25000
1006.20	0.004	68000	29 ms	-
1086.44	0.11	69000	827 µs	4500
1163.18	0.24	61000	360 µs	2100
1234.49	1.49	74000	65 µs	330
1317.27	0.33	60000	237 µs	1500
1357.49	1.37	75000	61 µs	360
1429.06	0.73	63000	104 µs	680
1527.46	0.06	66000	800 µs	8300
1529.25	1.88	62000	43 µs	260
1619.86	0.82	74000	70 µs	600
1643.96	1.28	68000	50 µs	400
1725.08	0.72	79000	68 µs	700
1762.63	2.25	70000	30 µs	200
1767.80	0.82	73000	63 µs	600
1800.69	0.22	76000	192 µs	2270
1869.62	0.10	76000	349 µs	5000
1890.12	0.73	64000	72 µs	700
1978.98	0.23	78000	162 µs	2200
1985.50	0.18	96000	165 µs	2800

Table IIIb Rise times of the quadrupole modes (nose cone cavity)

ω_r(MHz)	R/Q	Q_o	$\tau_{2,eff}$	Q (500 Ω)
703.66	4.03	30000	165 µs	120
1077.55	0.26	57000	448 µs	1900
1115.39	0.19	42000	755 µs	2600
1157.49	0.05	46000	2.5 ms	10000
1297.38	0.23	56000	365 µs	2200
1378.90	0.30	51000	273 µs	1650
1433.23	0.43	62000	160 µs	1150
1461.22	1.40	40000	77 µs	360
1526.02	1.01	73000	64 µs	500
1550.47	0.14	50000	473 µs	3550
1627.80	0.19	58000	295 µs	2600
1666.86	1.03	54000	68 µs	500
1755.69	0.80	52000	81 µs	600
1775.06	3.28	58000	25 µs	150
1807.09	0.35	37000	223 µs	1400
1910.56	1.53	57000	46 µs	300
1981.76	0.02	132000	905 µs	25000
1996.56	0.91	61000	59 µs	550
2060.52	0.53	60000	90 µs	950
2316.24	1.09	65000	45 µs	500
2409.98	2.09	65000	27 µs	250
2492.12	2.67	67000	21 µs	180
2617.94	0.91	50000	63 µs	550
2673.27	2.55	71000	23 µs	200

3. Longitudinal Landau Damping

Due to the non-linearity of the RF voltage, and in general, of the induced wake fields, the incoherent synchrotron frequency varies within the bunch. By rearranging the equation of the coherent frequency shift we get the following dispersion relation integral:

$$1 = j\frac{m\alpha_c I_o}{(E/e)\omega_s}\frac{Z(p)}{p}\int_o^\infty \frac{\partial g_o}{\partial \tau}\frac{J_1^2(p\omega_o\tau)}{\left[\omega_{cm} - m\omega_s(\tau)\right]} \tag{27}$$

Because of the non-linearity provided by the RF, there is a dispersion of synchronous frequency ω_s around ω_{so}:

$$\omega_s(\tau) = \omega_{so}\left[1 - \left(\frac{h\omega_o}{4}\right)^2 \tau^2\right] \tag{28}$$

with *h* harmonic number.

Then, assuming a Gaussian bunch, for the dipole mode *m*=1, we define:

$$G^{-1}(y) = \frac{2}{(p\omega_o\sigma_\tau)^2}\int_o^\infty \frac{Exp(-x)J_1^2(p\omega_o\sigma_\tau\sqrt{2x})}{x-y} \tag{29}$$

with

$$y = \frac{8\omega_{c1}}{\omega_{so}(h\omega_o\sigma_\tau)^2} \tag{30}$$

The stability limit is found by imposing Im(ω_{c1})->0, (or Im(y)->0). The corresponding impedance is:

$$Z_i(p) = \frac{\pi(h\omega_{so}\sigma_\tau)^2(E/e)}{2p\alpha_c I}\left[\frac{G_r(y)}{G_{ro}}\right] \tag{31}$$

$$Z_r(p) = \frac{-\pi(h\omega_{so}\sigma_\tau)^2(E/e)}{2p\alpha_c I}\left[\frac{G_i(y)}{G_{ro}}\right] \tag{32}$$

where $G_{ro} = G_r(y=0)$.

The resulting stability diagram is shown in Fig. 5

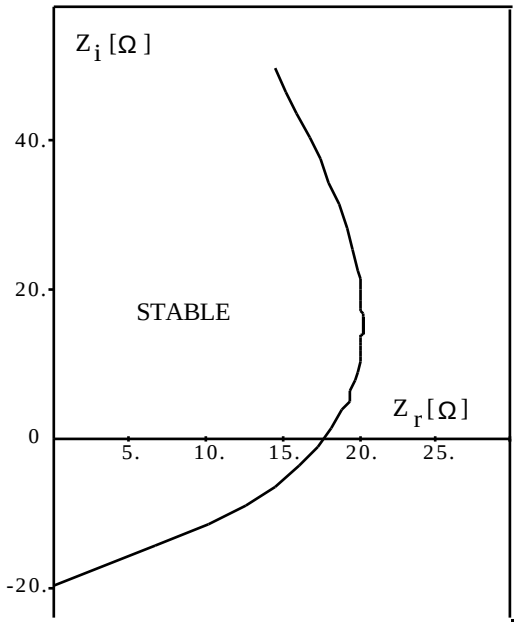

Fig. 5 - Stable region for the dipole mode (p=500).

One can see that a shunt impedance less than 17Ω would be required to keep the beam stable. For many HOM's, and expecially for the TM_{011}, such a strong requirement cannot be easily satisfied, even after a very strong damping. Accordingly, we do not expect any beneficial effect of Landau damping on the dipole oscillations for which we shall rely only on the feed-back system.

For the quadrupole mode m = 2, we define:

$$G^{-1}(y) = \frac{16}{(p\omega_o\sigma_\tau)^4} \int_o^\infty \frac{Exp(-x)J_2^2(p\omega_o\sigma_\tau\sqrt{2x})}{x-y} \qquad (33)$$

The stability limit is found by imposing $Im(\omega_{c2})$->0, (or $Im(y)$->0). The corresponding impedance is:

$$Z_i(p) = \frac{4\pi(h\omega_{so})^2(E/e)}{p^3\omega_o^2\alpha_c I}\left[\frac{G_r(y)}{G_{ro}}\right]_{m=2}$$

(34)

$$Z_r(p) = \frac{-4\pi(h\omega_{so})^2(E/e)}{p^3\omega_o^2\alpha_c I}\left[\frac{G_i(y)}{G_{ro}}\right]_{m=2}$$

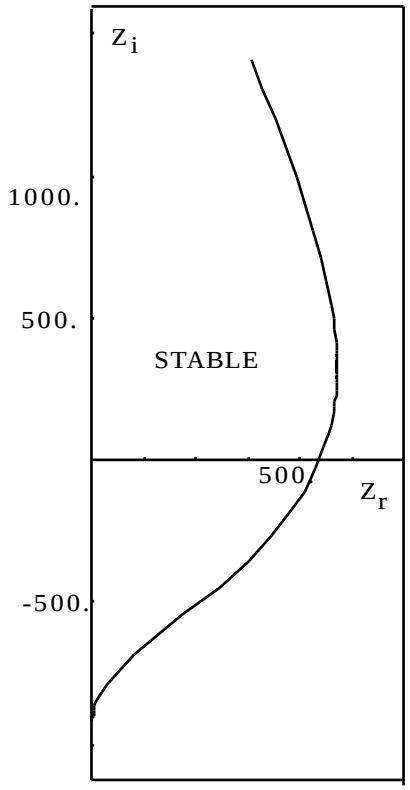

Fig. 6 - Stable region for the quadrupole mode (p=500).

The stability diagram shows that for the quadrupole relative mode it is necessary to keep the shunt impedance of the HOM's below 500 Ω if we want the Landau damping to be effective. In table IIIa and IIIb we give the maximum Q's allowed to keep the shunt impedance below this stability threshold. One can note that only the TM_{011} and few other parasitic modes have to be significantly damped.

It is worth to remind that the above calculations depend strongly on the bunch distribution. In fact if the bunch remains gaussian it is necessary to include the nonlinearities of the self field; on the other side a parabolic bunch does not introduce any linearity, but changes significantly the incoherent synchronous frequency. Accordingly a more accurate analysis of the single bunch effects in DAΦNE is in progress to work out a reliable calculation of Landau damping.

4. Transverse Multibunch Instabilities

Analogously to the longitudinal case we consider a single transverse relative mode, (m = 0 is the lowest one) coupled to a transverse resonance

$$Z_{\perp}(p) = \left(\frac{\omega_r}{\omega}\right) \frac{R'_{\perp}}{1 + jQ\left(\frac{\omega}{\omega_r} - \frac{\omega_r}{\omega}\right)} \qquad (35)$$

where

$$R'_{\perp} = \frac{R}{k_r a^2} = k_r R_{\perp}^{Urmel} \tag{36}$$

The coherent frequency shift is:

$$\omega_{co}^{\perp}(p) = -j\beta_{\perp} Z_{\perp}(p)\theta_o^{\perp}(p) \tag{37}$$

where $\beta_{\perp}$ is the beta function at the RF position and

$$\theta_o^{\perp}(p) = -\frac{I\omega_o}{4(E/e)} \int_o^{\infty} J_o^2\left\{((p+Q)\omega_o + \omega_{\xi})\tau\right\} g_o(\tau) d\tau \tag{38}$$

In the full coupling condition one usually gets:

$$\beta_{\perp}\theta_o^{\perp}(p) R'_{\perp} = \frac{1}{\tau_o^{\perp}} \tag{39}$$

Whereas the coherent frequency shift is obtained by solving the following approximate equation:

$$\omega_{co}^2 - j\alpha\omega_{co} + \frac{\alpha}{\tau_o^{\perp}} = 0 \tag{40}$$

which gives:

$$\omega_{co}^{\perp} = j\frac{1}{2\tau_f}\left(1 - \sqrt{1 + 4\frac{\tau_f}{\tau_o^{\perp}}}\right) \tag{41}$$

Again we find two regimes:

$$\tau_o^{\perp} >> \tau_f \qquad \omega_{co}^{\perp} \approx j\frac{1}{\tau_o^{\perp}} \tag{42}$$

$$\tau_o^{\perp} << \tau_f \qquad \omega_{co}^{\perp} \approx j\frac{1}{\sqrt{\tau_f \tau_o^{\perp}}} \tag{43}$$

Round shape - MM mode type:

ω_r(MHz)	$\frac{R/Q}{(k_r\ a)^2}$	Q_o	$\tau_{t\text{- eff}}$	Q_{loaded} $\tau_{t\text{- eff}}$=1ms
533.7	5.1	55500	165.0 µs	9200
784.24	3.41	46600	220.0 µs	10000
889.25	1.64	58000	320.0 µs	18000
928.88	0.004	75500	82.0 ms	
1056.18	0.137	51800	3.2 ms	
1190.19	0.01	50700	38.0 ms	
1254.9	0.294	67000	1.0 ms	
1343.06	0.079	53900	4.0 ms	
1457.4	0.013	53900	22.0 ms	
1545.27	0.019	64800	12.0 ms	
1598.28	0.065	69500	3.2 ms	
1687.17	0.009	170000	10.0 ms	
1696.83	0.004	77200	46.0 ms	
1737.94	0.029	89300	5.2 ms	
1804.48	0.026	96700	5.2 ms	
1823.95	0.104	90000	1.3 ms	
1918.93	0.02	71700	6.8 ms	
1950.42	0.006	82000	28.0 ms	
1969.88	0.149	97400	1.0 ms	
2005.38	0.052	122000	2.0 ms	
2056.69	0.001	82700	140.0 ms	
2084.4	0.005	78100	30.0 ms	
2146.33	0.122	109700	8.0 ms	
2190.73	0.005	78200	28.0 ms	
2318.65	0.002	82200	62.0 ms	
2341.16	0.075	104500	1.3 ms	
2366.44	0.003	141400	24.0 ms	
2441.7	0.012	84600	10.0 ms	
2522.41	0.026	113100	4.0 ms	
2537.47	0.005	152600	12.0 ms	
2549.47	0.014	102000	6.0 ms	
2601.48	0.028	69500	5.0 ms	
2709.48	0.011	148000	5.2 ms	

Round shape - EM mode type:

ω_r(MHz)	$\frac{R/Q}{(k_r\ a)^2}$	Q_o	$\tau_{t\text{- eff}}$	Q_{loaded} $\tau_{t\text{- eff}}$=1ms
530.98	16.1	52100	104.0 µs	5400
782.20	1.27	54400	720.0 µs	39000
961.84	0.23	51100	3.8 ms	
998.32	0.064	74850	9.5 ms	
1116.38	0.065	52200	13.5 ms	
1236.21	0.035	56700	22.0 ms	
1288.08	0.249	55600	3.5 ms	
1326.75	0.014	73900	44.0 ms	
1382.65	0.19	66500	3.8 ms	
1423.82	0.168	69500	4.0 ms	
1531.25	0.04	64300	18.5 ms	
1603.19	0.02	107400	4.0 ms	
1629.36	0.002	121700	200.0 ms	
1666.94	0.006	65000	120.0 ms	
1710.5	0.148	78800	4.0 ms	
1796.89	0.004	76700	160.0 ms	
1865.73	0.156	93200	3.5 ms	
1935.49	0.004	103600	120.0 ms	
1948.34	0.001	166200	335.0 ms	
1980.67	0.002	73800	340.0 ms	
2044.17	0.103	102700	4.8 ms	
2098.55	0.006	70600	120.0 ms	
2155.26	0.002	137600	185.0 ms	
2226.02	0.02	114400	22.0 ms	
2285.89	0.053	102750	9.5 ms	
2313.24	0.004	122900	218.0 ms	
2342.35	0.007	84000	88.0 ms	
2369.31	0.038	108300	12.0 ms	
2431.71	0.001	129400	400.0 ms	
2441.99	0.056	97900	10.0 ms	
2465.92	0.056	96700	10.0 ms	
2519.24	0.007	78800	92.0 ms	
2632.36	0.051	131250	8.0 ms	

Nose cone shape - MM mode type:

ω_r(MHz)	$\frac{R/Q}{(k_r\ a)^2}$	Q_o	$\tau_{t\text{- eff}}$	Q_{loaded} $\tau_{t\text{- eff}}$=1ms
655.84	0.85	40800	1.25 ms	
756.84	2.94	33300	410.0 µs	1360
924.86	0.609	44000	1.3 ms	
1048.57	0.21	61200	2.6 ms	
1104.06	0.04	54900	15.0 ms	
1232.4	0.077	47500	8.8 ms	
1352.46	0.002	44900	355.0 ms	
1441.82	0.15	41400	5.0 ms	
1481.83	0.05	50900	12.5ms	
1555.9	0.018	107300	16.5 ms	
1608.15	0.001	63400	500.0 ms	
1634.82	0.003	67100	160.0 ms	
1739.16	0.034	69200	13.8 ms	
1798.52	0.042	75000	10.0 ms	
1876.74	0.056	72000	8.0 ms	
1974.6	0.053	82000	7.5 ms	
1985.38	0.002	141500	118.0 ms	
2018.93	0.026	96700	13.5 ms	
2044.25	0.001	112400	298.0 ms	
2153.28	0.071	10800	4.7 ms	

References

[1] Sacherer, CERN/SI-BR/72-5 (1972).
[2] For instance, see, J.M. Wang, C. Pellegrini, Proceedings of the XI International High Energy Accelerators, Geneva, 1980.
[3] J.C. Laclare, CERN Accelerator School: Advanced Accelerator Physics, Oxford 1985, CERN 87-03, Vol. I, p.264.
[4] A. Hoffmann, B. Zotter, private communication.
[5] M.Bassetti, A. Ghigo, M.Migliorati, L.Palumbo, M.Serio, L.Verolino, "A Time domain simulation code for longitudinal multibunch instabilities", in preparation.
[6] M. Bassetti, O. Coiro, A. Ghigo, M. Migliorati, L. Palumbo, M. Serio, "DAΦNE Longitudinal feedback", Proceedings of EPAC'92.